Journal of Power Sources, 32 (1990) 287 - 301

NEW ZINC AND IRON ELECTRODES OF THE SECOND KIND IN SULPHURIC ACID, HYDROFLUORIC ACID AND (CYCLO)ALKYLAMMONIUM HYDROGEN SULPHATES

F. BECK*, H. KROHN, S. RASHWAN and I. LITZENBERGER

Universität GH Duisburg, FB 6 Elektrochemie, Lotharstrasse 1, D 4100 Duisburg 1 (F.R.G.)

(Received February 20, 1990; in revised form April 2, 1990)

Summary

New zinc and iron electrodes of the second kind have been examined in solutions of low pH. The electrolytes are 5 - 14 M H_2SO_4, 40 - 60% H_2F_2 and 3 - 5 M (cyclo)alkylammonium hydrogen sulphates in water, methanol or acetonitrile. The cyclic behaviour of the metals (as a layer on glassy carbon) under galvanostatic conditions (j = 1 - 10 mA cm^{-2}) has been investigated in detail.

Optimum results are found with some of the amine salt systems. Morpholinium hydrogen sulphate allows smooth cycling of zinc up to 60 cycles. No passivation in the anodic halfcycle is observed. The corrosion current density is only 10 μA cm^{-2}. Current efficiency for the electroplating of zinc in the cathodic halfcycle is high. A potential difference of about 300 mV between charge and discharge indicates the presence of a protective layer. Tendency for passivation is a general problem, especially for iron, and it has been studied in greater detail. The results are interpreted in terms of a salt-like layer rather than an oxide film.

1. Introduction

Metal electrodes of the second kind are frequently employed as negatives in electrochemical power sources. Traditional aqueous systems, namely $Pb/PbSO_4/H_2SO_4$ or $Cd/Cd(OH)_2/KOH$ have a high practical potential [1, 2]. However, they are unsatisfactory due to a low chemoelectric equivalent, complicated manufacturing processes and serious environmental drawbacks. A system based on zinc or iron in acid to neutral electrolytes would be therefore highly welcome. Their compatibility with oxide and graphite

*Author to whom correspondence should be addressed.

0378-7753/90/$3.50

intercalation electrodes would be faciliated. Besides alkaline zinc and iron electrodes, only the Leclanché system $Zn/ZnCl_2/NH_4Cl$ is known as a possible (primary) alternative in slightly acid solutions. Early attempts to employ heavily amalgamated zinc as a negative in the lead acid accumulator [2, 3] were totally abandoned later.

It is the objective of this work to report on the electrochemical behaviour of zinc and iron electrodes in concentrated solutions of sulphuric acid, hydrofluoric acid and (cyclo)alkylammonium hydrogen sulphates.

2. Experimental

The reagents used were as follows: sulphuric acid (97%, Merck) was AnalaR grade, 70% HF (Riedel de Haen) was of purum quality. The amines ('for synthesis') were freshly distilled. Concentrated solutions of amine salts in water or methanol were prepared by slowly mixing equimolar portions of the amine with the acid in the solvent at about 0 °C (cf. Tables 1 to 3 and 5 to 7). Saturation of the electrolyte with $ZnSO_4 \cdot 1H_2O$ or $FeSO_4 \cdot 1.5H_2O$ was performed in most of the measurements. The electrodes were 10 μm thick layers of pure zinc or iron electrodeposited on a lightly sandblasted glassy carbon disc (GC) from a metal sulphate/$(NH_4)_2SO_4$ electrolyte at 60 - 70 °C [4]. The peripheral parts of the glassy carbon disc were not sandblasted to ensure the sealing of the O-ring. Current efficiency (from gravimetric measurements) was 98% for Zn and 92% for Fe, respectively.

The plated electrode was inserted into the electrochemical cell as shown in Fig. 1. The plated surface area was 1.3 cm^2. The cell indicated was also used for all standard measurements. The horizontal working electrode prevented product layers developing on the surface of the electrode from shedding. The holder for the plated glassy carbon disc electrode has been previously described [5]. All measurements were performed at 20 °C in unstirred electrolytes and under an argon atmosphere. The reference electrode was $Hg/Hg_2SO_4/1\ M\ H_2SO_4$ (674 mV *versus* SHE); potentials measured against this reference are denoted as U_s.

The experimental apparatus consisted of an AMEL 545 bigalvanostat, an Indigel timer and an AMEL 868 voltage/time recorder. Analogous equipment was used in our previous measurements at graphite intercalation electrodes [6]. At the beginning of the most important galvanostatic alternating polarization (GAP) experiment, anodic polarization at 1 mA cm^{-2} was performed for 10 min. The anodic conversion of the metal layer was only 2.5%. Thereafter, the current was reversed for another 10 min to achieve eventual redeposition of the metal. Twenty cycles were employed to test the battery electrode behaviour.

Slow cyclic voltammetry at the metal electrodes was performed at 10 mV s^{-1} with the usual standard potentiostatic equipment. Corrosion experiments were evaluated by mass loss determination and by corrosion potential/time curves up to the total dissolution of the metal layer.

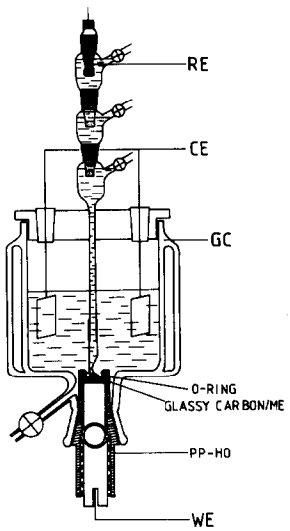

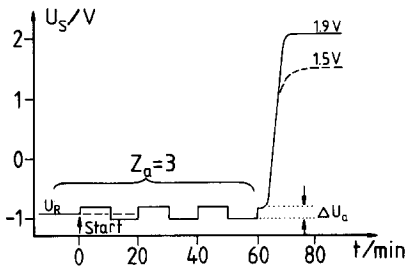

Fig. 1. Electrochemical cell with horizontal working electrode WE. GC: glass cell, thermostated; CE: two counter electrodes; RE: reference electrode; PP-HO: electrode holder made of polypropylene.

Fig. 2. Schematic representation of a GAP experiment with three active cycles ($Z_a = 3$). U_R = rest potential; ΔU_a = potential difference between anodic and cathodic part of the cyclic curve.

3. Results and discussion

3.1. Evaluation of GAP experiments

The performance has been already described in Section 2. Figure 2 shows a schematic representation of the potential time behaviour as a result of galvanostatic cycling at a current density of 1 mA cm^{-2}. In the *ideal* case, the electrode remained active for the preset 20 cycles ($Z_a = 20$), the mass balance was virtually zero ($\Delta m = 0$) and the potential difference between the charge and discharge potential was relatively low ($\Delta U_a < 100$ mV). However, in many cases a 'passivation phenomenon' was observed. After Z_a active cycles ($Z_a = 3$ in the example given in Fig. 2), the potential rose appreciably in the course of the next anodic polarization cycle and a new steady state anode potential level was established, e.g. $U_s = 1.5$ V for the blank glassy carbon or $U_s = 1.9$ V for the passive zinc electrode in H_2SO_4. ΔU_a was larger in these cases, but also in those where a stable electrode of the second kind could be realized. A mass loss of $\Delta m = -5.2$ mg would be measured after 20 cycles, if zinc was only dissolved anodically and not redeposited cathodically; the zinc salt was removed in the rinsing procedure. For Δm between 0 and -5.2 mg, a redeposition with a less than 100% current efficiency and/or slight corrosion must be assumed. For $\Delta m > 5.2$ mg, heavy corrosion must be occurring. The surface of the zinc after cycling may appear unattacked ('me') or have a surface oxide film ('ox'). The following Tables must be read in the light of this nomenclature.

3.2. Aqueous sulphuric acid

Both zinc and iron corrode heavily in dilute sulphuric acid, and they tend to passivate at higher concentrations. The question arises: can an intermediate state be found suitable for battery application? Table 1 illustrates our results for 5 - 14 M H_2SO_4; it was not possible to find such a state at these concentrations.

At concentrations above 9 - 10 M, both metals passivate even within the first cycle and Δm is negligible. Figure 3 shows some interesting details for iron in 12 M H_2SO_4. In the course of the early cycles, the Fe^{2+}/Fe^{3+} potential ($U_s \sim 0.1$ V) is repeatedly established. Typical potential oscillations are observed. In later cycles the electrode potential is stable at about 1.5 V, but the glassy carbon remains coated and Δm is virtually zero.

In more diluted H_2SO_4, a few active cycles are followed by cycles where only Fe^{2+}/Fe^{3+} redox cycles occur at the surface of the blank glassy carbon (see Fig. 4).

The transition of the active cycling to passivation is strongly correlated with the solubility of $FeSO_4$. It was determined to be 100, 3, 0.5, 0.3 and 0.1 g $FeSO_4$ per dm^3 in 8, 9, 10, 12 and 14 M H_2SO_4, respectively. In 12 M H_2SO_4, other current densities than 1 mA cm^{-2} were examined. Lower levels of j lead to reactivation, with a subsequent dissolution of the metal. Higher current densities forced the system to deposit iron from the solution, cf. Table 1.

Similar behaviour was found for zinc electrodes. Table 1 shows that passive behaviour is found at concentrations $\geqslant 9$ M, while in 8 M H_2SO_4 active cycles begin to occur for the first time. Figure 5 displays the GAP

TABLE 1

GAP results for Fe and Zn in 5 - 14 M H_2SO_4, $j = \pm 1$ mA cm^{-2}. The electrolytes were saturated with $FeSO_4$ and $ZnSO_4$, respectively

Me	H_2SO_4 (M)	$U_{R,S}$ (V)	ΔU_a (mV)	Z_a	Δm (mg)	Residual layer
Fe	14	−0.9		0	0	ox
	12	−0.95		0	0	me
	12[a]	−0.95	10	1	−10	ox
	12[b]	−0.9	—	0	+10	me
	10	−0.9	—	0	0	
	9	−1.0	20	2	−7	ox
	8	−1.0	20	4	−10	
	5	−0.95	50	5	−9.6	
Zn	14	−1	—	0	−1	me
	12	−1.1	—	0	−1	me
	10	−1.3	—	0	−3	me
	9	−1.3	—	0	−7	me
	8	−1.44	10	2	−10	
	5	−1.45	10	5	−10	

[a] $j = 0.03$ mA cm^{-2}.
[b] $j = 3$ or 10 mA cm^{-2}.

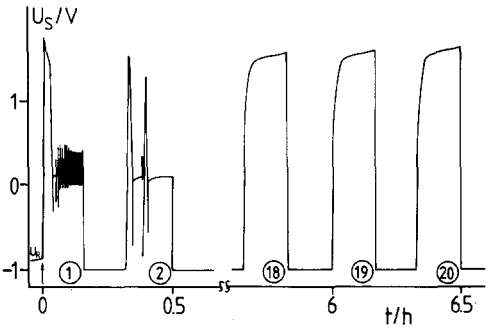

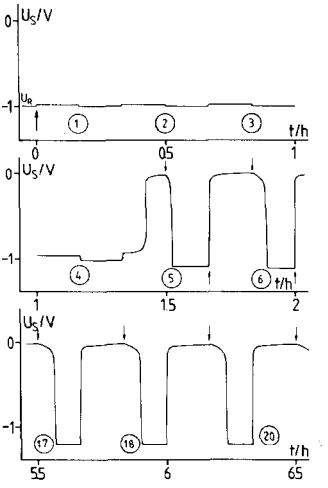

Fig. 3. GAP curve ($j = \pm 1$ mA cm^{-2}) for Fe/GC in 12 M H_2SO_4, $FeSO_4$ sat.

Fig. 4. GAP curve ($j = \pm 1$ mA cm^{-2}) for Fe/GC in 8 M H_2SO_4, $FeSO_4$ sat. The arrows indicate the points of current reversal.

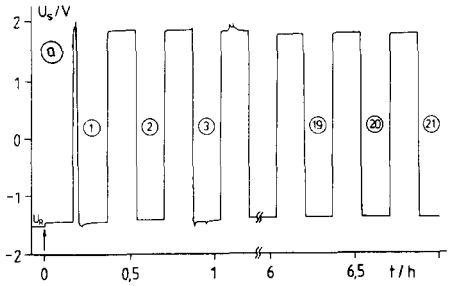

Fig. 5. GAP curve ($j = \pm 1$ mA cm^{-2}) for Zn/GC in 10 M H_2SO_4, $ZnSO_4$ sat.

curve in 10 M H_2SO_4. The passive state is reproducible in agreement with our previous findings [7].

At lower concentrations, the zinc inventory is consumed via corrosion after a few cycles. We could not confirm the statement of Hedges [8] that passivation occurs even in 5 M H_2SO_4.

3.3. Sulphuric acid in water with cosolvents

We have repeated the GAP measurements in 8 M H_2SO_4 in the presence of various co-solvents. In aqueous 8 M H_2SO_4, corrosion was dominant for both metals. An improvement could be observed for 70% acetonitrile or 90% methanol, but only for iron, cf. Table 2. An aged solution of 8 M H_2SO_4 in MeCN increased the tendency for passivation. This may be due to the acetic acid, which is formed via saponification. Acetic acid alone led to a total passivation. Caution: a mixture of 97% H_2SO_4 and pure acetonitrile may explode! Figure 6 shows an example for a GAP curve of Fe in a pristine solu-

TABLE 2

GAP results for Fe and Zn in 8 M H_2SO_4 in mixed solvents, $j = \pm 1$ mA cm^{-2}. The electrolytes were saturated with $FeSO_4$ and $ZnSO_4$, respectively

Me	Solvent	$U_{R,S}$ (V)	ΔU_a (mV)	Z_a	Δm (mg)	Residual layer
Fe	H_2O	−1.0	20	4	0	ox
	90% MeCN	−0.89	60	12	−5	ox
	70% MeCN (freshly prepared)	−0.83	250	20	−9	me
	70% MeCN (aged)	−0.81	340	5	+1	me
	90% MeCOOH	−0.82		0	0	ox
Zn	H_2O	−1.44	10	2	−10	me
	90% MeOH	−1.37	50	7	−10	me
	70% MeCN (freshly prepared)	−1.37	45	3	−10	

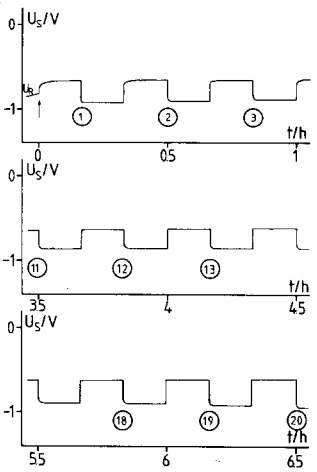

Fig. 6. GAP curve ($j = \pm 1$ mA cm^{-2}) for Fe/GC in 8 M H_2SO_4, 70% CH_3CN (freshly prepared solution), $FeSO_4$ sat.

tion of 8 M H_2SO_4 in 70% MeCN. Even there, a slight increase of ΔU_a was observed in the course of the 20 cycles.

A medium ΔU_a value of about 300 mV is observed for the first time. It seems to be indicative of a ion permeable surface layer at the metal surface which can be considered as a protective layer against corrosion.

3.4. Aqueous hydrofluoric acid

Table 3 compiles the GAP results for iron and zinc in 40 and 60% HF at two current density levels. The measurements were performed in a cell fabricated from polypropylene. Corrosion and anodic passivation is a severe problem in nearly all cases. The only exception is with zinc in 40% HF at 1 mA cm^{-2}, where 20 active cycles could be achieved. As shown in Fig. 7,

TABLE 3

GAP results for Fe and Zn in H_2F_2. The electrolytes were saturated with FeF_2 and ZnF_2, respectively

Me	H_2F_2 (wt.%)	j (mA cm^{-2})	$U_{R,S}$ (V)	ΔU_a (mV)	Z_a	Δm (mg)	Residual layer
Fe	40	1	−0.97	10	1	+5	
	40	10	−0.95		0	−6	
	60	1	−0.95		0	−7	
	60	10	−0.95		0	−10	
Zn	40	1	−1.35	50	20	−6	ox
	40	10	−1.36	75	8	−8	
	60	1	−1.32	25	9	−9	
	60	10	−1.33	75	2	−9	

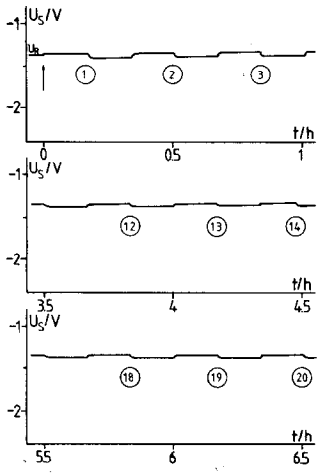

Fig. 7. GAP curve (j = ±1 mA cm^{-2}) for Zn/GC in 40% H_2F_2, ZnF_2 sat.

cycling is very smooth under these conditions, and ΔU_a remains very low. However, corrosion is again relatively high, cf. Table 3. In addition, environmental impacts of this electrolyte are not negligible. It was for both reasons that further development of an HF electrolyte was cancelled.

3.5. (Cyclo)alkylammonium hydrogen sulphates

We have found that for the free acids corrosion played a predominating role in the course of the active cycles. We employed, therefore, stoichiometric amounts of (cyclo)aliphatic amines to yield the corresponding alkylammonium salts. Table 4 compiles some solubility data for these salts in water and methanol and for $FeSO_4$ and $ZnSO_4$ in 5 M aqueous amine salt solutions.

It can be seen that the solubility in water and methanol is much higher than that of the alkali hydrogen sulphates (the sodium salt is given as an

TABLE 4

Solubility (c_s) data (c_s in g/100 g solvent) for amine hydrogen sulphates in water (A) and methanol (B) and for $FeSO_4 \cdot 1.5H_2O$ (C, D) and $ZnSO_4 \cdot H_2O$ (E, F) in 5 M solutions of these amine salts in water and methanol, respectively

Base	A (H_2O)	B (MeOH)	$FeSO_4 \cdot 1.5H_2O$		$ZnSO_4 \cdot H_2O$	
			C (H_2O)	D (MeOH)	E (H_2O)	F (MeOH)
Triethylamine	45	117	0.5	0.5	0.3	0.5
n-Butylamine			0.5	0.5	0.5	0.5
Morpholine	1500	350	1	0.5	2.5	0.5
Piperidine	470	380				
Pyridine	1200	370				
NaOH	21	0.04				

example). Acetonitrile is, however, a poor solvent (about 1 g amine salt per 100 g MeCN). Solubilities of zinc and iron sulphate are low enough to allow for the formation of electrodes of the second kind. For pure morpholinium hydrogen sulphate and butylammonium hydrogen sulphate, we observed a viscous oil at room temperature, which solidifies only at 0 °C. This is another example of an organic salt melt at room temperature, of which the imidazolium salts [9, 10] and *N*-butylpyridinium salts [11, 12] are well known systems. The electrochemical behaviour of alkylammonium chloride and other amine salts as low temperature salt melts was extensively studied by Kisza *et al.* [13 - 15]. However, no salt melts at room temperature were found for these systems.

In the case of triethylamine, the acid base equilibrium

$$NEt_3 + H_2SO_4 \rightleftharpoons NEt_3H^+ + HSO_4^- \quad (1)$$

is shifted to the right, thus allowing an appreciable decrease in the acidity of the system. Table 5 illustrates results for GAP experiments performed in six different amine salt electrolytes. The concentration of these was in the order of 5 M. Amine, sulphuric acid and solvent were mixed in the mole ratios 1:1:1.53 for water and 1:1:1.39 for methanol, corresponding to volume ratios of salt:solvent of 2:1 in both cases.

The system with morpholinium hydrogen sulphate in methanol proved to be the optimum. Twenty active cycles could be achieved, and weight loss of zinc was only about 4 mg. Figure 8 shows parts of the GAP curves. Again, ΔU_a is medium due to the formation of a protective layer; Δm could not be reduced by increasing the cathodic current densities to 3 or 7.7 mA cm^{-2} (for 3.3 or 1.7 min duration). However, the ΔU_a values were strongly enhanced to 750 and 1000 mV (Fig. 9). This indicates a high resistivity for the protective layer. However, the example in Fig. 13 demonstrates that ΔU_a is reduced upon dilution of the electrolyte concentration to 3 M. Prolongation of the charging time to 30 min increased the tendency of an early passivation, and this point will be further discussed in Section 3.8.

TABLE 5

GAP results for Zn in ~5 M alkylammonium hydrogen sulphates in water and methanol (see text). The electrolytes were saturated with $ZnSO_4 \cdot H_2O$; $j = \pm 1$ mA cm^{-2}

Amine	Solvent	$U_{R,S}$ (V)	ΔU_a (mV)	Z_a	Δm (mg)	Residual layer
n-Butylamine	H_2O	−1.37	150	20	−10	me
	MeOH	−1.37	170	3	0	me
Morpholine	H_2O	−1.4	200	20	−6	me
	MeOH[a]	−1.35	250	20	−3.6	me
	MeOH[a]	−1.37	270	20	−4.1	me
Piperidine	H_2O	−1.35	270	20	−6.3	me
Trimethylamine[b]	H_2O	−1.4	100	16	−9.9	
Triethylamine	H_2O	−1.35	400	2	0	me
	MeOH	−1.37		0	−3	me
Pyridine	H_2O	−1.39	150	20	−9.2	me
[5 M H_2SO_4]	H_2O	−1.45	10	5	−10	

[a]Two parallel runs to check reproducibility.
[b]Mole ratio $NMe_3H^+HSO_4^-$:H_2O = 1:3.2.

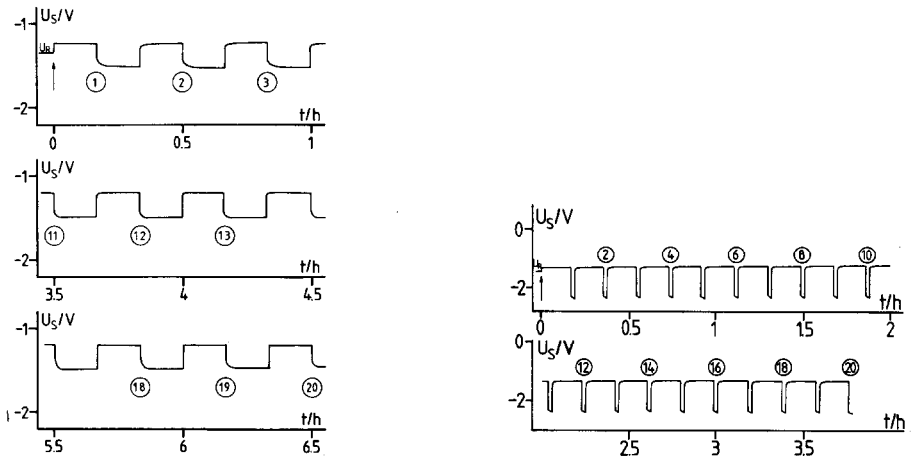

Fig. 8. GAP curve ($j = \pm 1$ mA cm^{-2}) for Zn/GC in 5 M morpholinium hydrogen sulphate in methanol, $ZnSO_4$ sat.

Fig. 9. GAP curve for Zn/GC at various current densities; anodic +1 mA cm^{-2} for 10 min and cathodic −10 mA cm^{-2} for 1.3 min. The electrolyte was 5 M morpholinium hydrogen sulphate in methanol, $ZnSO_4$ sat.

Analogous GAP experiments with iron layers revealed a stronger tendency to passivation in all cases. It was only with the aqueous morpholinium hydrogen sulphate that 20 active cycles could be achieved. The mass losses were about the same as for zinc.

3.6. Corrosion of zinc

Corrosion of zinc was measured gravimetrically or by recording the corrosion potential. After total dissolution of the zinc layer, a steep potential shift to the level of the glassy carbon potential was observed. Figure 10 gives an example for such a curve. The corrosion current densities so derived are compiled in Table 6. The corrosion rate in 5 or 8 M H_2SO_4 is 3 to 5 orders of magnitude higher than the corrosion rate in the alkylammonium hydrogen sulphate. However, the optimum performance in the GAP experiments does not coincide with the minimum corrosion rate. This may be due to anodically and even cathodically stimulated corrosion. Differences in cathodic zinc deposition efficiency must be noted as well, and this point will be further discussed in the following paragraph.

3.7. Electrodeposition of zinc

We have evaluated the current efficiency for the electrodeposition of zinc under the conditions of the GAP cycling experiments. The experiments at 1 or 3 mA cm^{-2} were designed to yield the electrodeposition of 10.0 mg of zinc onto the zinc coated GC-cathode, assuming 100% efficiency. The mass balance shown in Table 7 is therefore a direct measure of this current efficiency.

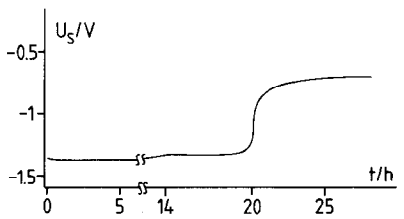

Fig. 10. Corrosion potential/time curve for a 10 μm Zn layer on GC. Corrosion medium: 5 M morpholinium hydrogen sulphate in water.

TABLE 6

Corrosion rates for 10 μm Zn layers on glassy carbon in various electrolytes

Electrolyte	Solvent	j_{corr} (mA cm^{-2})
5 M H_2SO_4	H_2O	15
8 M H_2SO_4	H_2O	21
5 M $NBuH_3^+HSO_4^-$	H_2O	0.15
	MeOH	0.0014
5 M Morpholinium–HSO_4^-	H_2O	0.22
	MeOH	0.29
5 M $NEt_3H^+HSO_4^-$	H_2O	0.006
	MeOH	0.00093
5 M Piperidinium–HSO_4^-	H_2O	0.039
5 M Pyridinium–HSO_4^-	H_2O	0.22

Table 7 demonstrates that corrosion is dominating in the free acid at a concentration of 5 and 8 M. In the amine salt solutions, a positive mass balance is found, and the current efficiency reaches about 80%. The results with morpholinium hydrogen sulphate reveal that dilution of the electrolyte and an increase in current density lead to a higher current efficiency (c.e.) for zinc electrodeposition. Substitution of water by methanol lowered the c.e. in this system, for the others a slightly improved c.e. was found.

3.8. Passivation of zinc

Due to the importance of passivation phenomena in the course of the cyclization of the zinc electrode, we have undertaken a separate investigation into its passivation in the electrolytes studied. The slow potentiodynamic

TABLE 7

Mass balance for the cathodic deposition of zinc onto GC/10 μm Zn from $ZnSO_4 \cdot H_2O$ saturated electrolytes. Δm = 10 mg corresponds to 100% current efficiency; j = 3 mA cm^{-2}

Electrolyte	Solvent	Δm (mg)
5 M H_2SO_4	H_2O	−10
8 M H_2SO_4	H_2O	−10
5 M $NBuH_3^+HSO_4^-$	H_2O	0
	MeOH	+1
5 M Morpholinium–HSO_4^-	H_2O	+3.7
	H_2O	+2.6[a]
	MeOH	+0.6
3 M Morpholinium–HSO_4^-	H_2O	+7.7
	H_2O	+4.8[a]
5 M $NEt_3H^+HSO_4^-$	H_2O	0
	MeOH	+1
5 M Pyridinium–HSO_4^-	H_2O	+1.4

[a] j = 1 mA cm^{-2}.

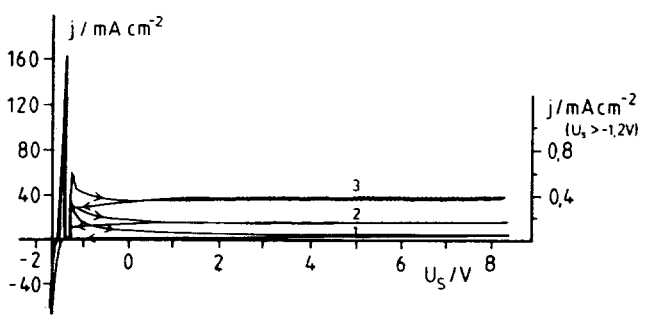

Fig. 11. Potentiodynamic current voltage curve (v_s = 10 mV s^{-1}) of zinc in 8 M H_2SO_4, $ZnSO_4$ sat., 3 cycles.

current voltage curve shows the usual active/passive transition. Figure 11 displays a characteristic example in 8 M H_2SO_4, $ZnSO_4$ sat. The active peak exceeds 100 mA cm^{-2}, and the current decreases sharply by three orders of magnitude in the passive region. We ascribe the increase of the corrosion current density j_c in the passive state upon cycling to a roughening effect. j_c decreases nearly linearly with increasing electrolyte concentration. The voltage scan was reversed at 8 V in the standard experiment. An extension to higher voltages revealed that a sudden steep rise of current occurred at only very high values $U_s > 50$ V. This seems to be a dielectric breakdown of the avalanche type. No oxygen evolution seems to be possible at the passivating layer, and j_c seems to be a space charge limited dissolution of the metal. Similar results were found by Maitak [16]. However, if the current is suddenly interrupted at a galvanostatically polarized zinc electrode, the passive potential breaks down immediately, and the active potential is established within less than 1 ms. This is quite in contrast to the normal behaviour, where the passive potential is maintained until the total dissolution of the layer at open-circuit potential, cf. ref. 17. We conclude that the passivating layer is of the monolayer type, dissolving in a very short time.

If a constant current is applied the electrode remains, for a time τ, in the active state, but then suddenly the potential rises steeply. τ is strongly dependent on j, and a Sand type behaviour

$$j\sqrt{\tau} = \text{constant} \tag{2}$$

is observed. The slope of the $\tau^{-1/2}$ *versus* j plot depends strongly on the concentration of the electrolyte, and Fig. 12 gives an example.

'Diffusion coefficients' D, derived from these experiments, with the aid of the Sand equation decay exponentially with the electrolyte concentration from 10^{-2} to 10^{-8} cm^2 s^{-1}. It is clear from these values that D is not due to the liquid phase. We feel that our experiments are controlled by the kinetics of phase formation. We have found current voltage behaviour and transients like those of Figs. 11 and 12 for all electrolytes described in this paper. Our results will be published in greater detail elsewhere [18].

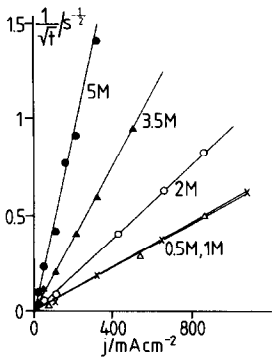

Fig. 12. $1/\sqrt{\tau}$ *vs.* j plots for the galvanostatic polarization of zinc in morpholinium hydrogen sulphate solutions of various concentrations.

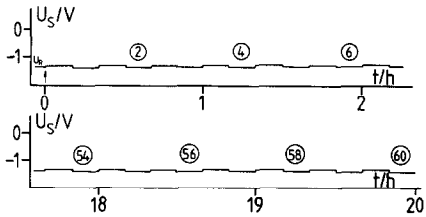

Fig. 13. GAP curve ($j = \pm 1$ mA cm^{-2}) for Zn (37.3 μm)/GC in 3 M morpholinium hydrogen sulphate in water. The experiment was extended to 60 cycles.

In accordance with these results, we have found that an extension of the standard GAP experiments to 60 cycles leads to very different results in all cases where the initial 20 cycles were active. From 11 experiments with different systems, only 4 could be extended to 60 cycles. Figure 13 displays one example. Interestingly, the mass loss was arbitrarily proportional to the number of active cycles, and this indicates very clearly the absence of any formation effects. For the other 7 trials, passivation occurred between the 20th and the 60th cycle. This result shows that even under the conditions of the GAP experiment, a transition time for the passivation is established. A memory effect for the anodic part of the curve must be assumed.

4. Conclusions

The cyclic behaviour of the zinc electrodes in contact with concentrated solutions of H_2SO_4, H_2F_2 and alkylammonium hydrogen sulphates is characterized by a complicated interaction between active/passive transitions, corrosion and electrodeposition. The main difference between our electrodes of the second kind and classical ones is the relative low value of the hydrogen overvoltage for zinc and iron. It is for this reason that a porous surface layer of the corresponding sparingly soluble salt is not sufficient as in the case of the $Pb/PbSO_4/H_2SO_4$ electrode for example, cf. Fig. 14. A thin, protective layer D is absolutely necessary, which is ionically conducting.

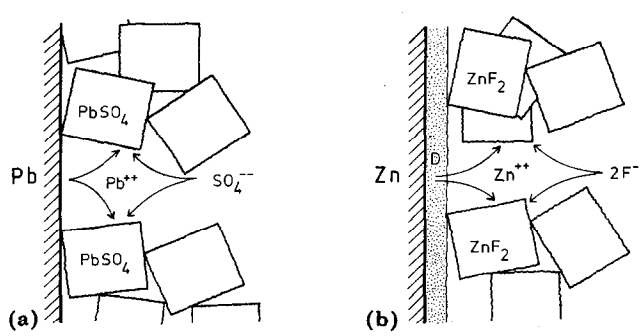

Fig. 14. Schematic representation of electrodes of the second kind: (a) $Pb/PbSO_4/H_2SO_4$; (b) $Zn/ZnF_2/H_2F_2$.

Moreover, it must meet the following conditions:

- no passivating properties
- low resistance
- an inhibitor for hydrogen evolution
- allowing redeposition of zinc

The situation resembles closely that for the lithium battery electrode, where salt like protective layers 'SEI' (solid electrolyte interphase) have been proposed to account for the cyclic behaviour [19, 20]. Other models for Li are based on a solid polymer electrolyte layer [21] or a dielectric layer [22]. Recently, the SEI model has been applied to the system calcium/thionyl chloride [23]. However, this experience can only partially be transferred to our problem, for we have mainly aqueous electrolytes, and larger ions like Zn^{2+} must migrate in the film.

It must be assumed that these films have some permeability for protons. As a consequence, proton activity must be lowered in the electrolyte. We made a first approach by the introduction of alkylammonium hydrogen sulphates. At the anion, a relatively acid proton remains, and we therefore studied the result of its removal in various alkylammonium salts of monobasic acids derived from S-VI [24].

Acknowledgement

Financial support of our work by the MWF (Ministry of Science and Research) of the country Northrhine Westphalia is gratefully acknowledged.

References

1 D. Linden (ed.), *Handbook of Batteries and Fuel Cells*, McGraw-Hill, New York, 1984.
2 F. Beck and K.-J. Euler, *Elektrochemische Energiespeicher*, VDE, Berlin, 1984.
3 E. J. Wade, *Secondary Batteries*, The Electrician Printing & Publishing Company, New York, 1902.
4 A. G. Gray, *Modern Electroplating*, Wiley, New York, 1953.
5 F. Beck and A. Pruss, *Electrochim. Acta*, *28* (1983) 1847.
6 F. Beck, H. Krohn and W. Kaiser, *J. Appl. Electrochem.*, *12* (1982) 505.
7 F. Beck and H. Krohn, *DECHEMA-Monograph.*, *92* (1982) 57.
8 E. S. Hedges, *J. Chem. Soc.*, (1926) 2580.
9 J. S. Wilkes, J. A. Levisky, R. A. Wilson and Ch. L. Hussey, *Inorg. Chem.*, *21* (1982) 1263.
10 A. A. Fannin, D. A. Floreani, L. A. King, J. S. Landers, B. J. Piersma, D. J. Stech, R. L. Vaughn, J. S. Wilkes and J. L. Williams, *J. Phys. Chem.*, *88* (1984) 2614.
11 F. H. Hurley and T. P. Wier, *J. Electrochem. Soc.*, *98* (1951) 203.
12 H. L. Chum and R. A. Osteryoung, in D. Inman and D. G. Lovering (eds.), *Ionic Liquids*, Plenum, New York, 1981, pp. 407 - 423.
13 A. Kisza and J. Hawranek, *Z. Phys. Chem.*, *237* (1968) 210.
14 A. Kisza, *Acta Phys. Pol.*, *34* (1968) 1063.

15 A. Kisza, in P. Franzosini and M. Sanesi (eds.), *Thermodynamic and Transport Properties of Organic Salts*, Pergamon, Oxford, 1980.
16 G. P. Maitak, *J. Appl. Chem. U.S.S.R., 31* (1958) 1488.
17 D. J. Blackwood and L. M. Peter, *Electrochim. Acta, 33* (1988) 1143.
18 S. Rashwan, H. Krohn and F. Beck, *J. Electroanal. Chem.*, submitted for publication.
19 E. Peled, *J. Electrochem. Soc., 126* (1979) 2047.
20 E. Peled, in J. P. Gabano (ed.), *Lithium Batteries*, Academic Press, New York, 1983, p. 600.
21 J. Thevenin, *J. Power Sources, 14* (1985) 45.
22 I. A. Kedrinsky, I. V. Murygin, V. E. Dmitrenko, O. E. Abolin, G. I. Shukova and I. I. Grudyanov, *J. Power Sources, 22* (1988) 99.
23 A. Meitav and E. Peled, *Electrochim. Acta, 33* (1988) 1111.
24 F. Beck, H. Krohn, S. Rashwan and D. Schleithoff, *J. Appl. Electrochem.*, submitted for publication.